



# A Novel Cre Recombinase-Mediated *In Vivo* Minicircle DNA (CRIM) Vaccine Provides Partial Protection against Newcastle Disease Virus

Yanlong Jiang,<sup>a</sup> Xing Gao,<sup>a</sup> Ke Xu,<sup>a</sup> Jianzhong Wang,<sup>a</sup> Haibin Huang,<sup>a</sup> Chunwei Shi,<sup>a</sup> Wentao Yang,<sup>a</sup> Yuanhuan Kang,<sup>a</sup> Roy Curtiss III,<sup>b</sup> Guilian Yang,<sup>a</sup> Chunfeng Wang<sup>a</sup>

<sup>a</sup>College of Animal Science and Technology, Jilin Provincial Engineering Research Center of Animal Probiotics, Key Lab of Animal Production, Product Quality and Security, Ministry of Education, Jilin Agricultural University, Changchun, China

<sup>b</sup>Department of Infectious Disease and Immunology, College of Veterinary Medicine, University of Florida, Gainesville, Florida, USA

**ABSTRACT** Minicircle DNA (mcDNA), which contains only the necessary components for eukaryotic expression and is thus smaller than traditional plasmids, has been designed for application in genetic manipulation. In this study, we constructed a novel plasmid containing both the Cre recombinase under the phosphoglycerate kinase (PGK) promoter and recombinant *lox66* and *lox71* sites located outside the cytomegalovirus (CMV) expression cassette. The strictly controlled synthesis of Cre recombinase *in vivo* maintained the complete form of the plasmid *in vitro*, whereas the *in vivo* production of Cre transformed the parental plasmid to mcDNA after transfection. The newly designed Cre recombinase-mediated *in vivo* mcDNA platform, named CRIM, significantly increased the nuclear entry of mcDNA, followed by increased production of mRNA and protein, using enhanced green fluorescent protein (EGFP) as a model. Similar results were also observed in chickens when the vaccine was delivered by the regulated-delayed-lysis *Salmonella* strain  $\chi$ 11218, where significantly increased production of EGFP was observed in chicken livers. Then, we used the HN gene of genotype VII Newcastle disease virus as an antigen model to construct the traditional plasmid pYL43 and the novel mcDNA plasmid pYL47. After immunization, our CRIM vaccine provided significantly increased protection against challenge compared with that of the traditional plasmid, providing us with a novel mcDNA vaccine platform.

**IMPORTANCE** Minicircle DNA (mcDNA) has been considered an attractive alternative to DNA vaccines; however, the relatively high cost and complicated process of purifying mcDNA dramatically restricts the application of mcDNA in the veterinary field. We designed a novel *in vivo* mcDNA platform in which the complete plasmid could spontaneously transform into mcDNA *in vivo*. In combination with the regulated-delayed-lysis *Salmonella* strain, the newly designed mcDNA vaccine provides us with an elegant platform for veterinary vaccine development.

**KEYWORDS** DNA vaccines, *Salmonella*-delivered vaccines, minicircle DNA

As a paramyxovirus, the Newcastle disease virus (NDV), with an enveloped membrane and nonsegmented negative-stranded RNA, poses a severe threat for poultry production (1). In particular, the dominant strain in China is the genotype VII NDV, which has resulted in significant economic loss for poultry production (2) since the most popular vaccine strains in the market belong to other genotypes, such as genotypes I, II, and III (3). Therefore, the demand for the development of novel NDV vaccines for genotype VII has received increasing attention recently.

Vaccines against NDV include the traditional inactivated virus, attenuated vaccines,

**Citation** Jiang Y, Gao X, Xu K, Wang J, Huang H, Shi C, Yang W, Kang Y, Curtiss R, III, Yang G, Wang C. 2019. A novel Cre recombinase-mediated *in vivo* minicircle DNA (CRIM) vaccine provides partial protection against Newcastle disease virus. *Appl Environ Microbiol* 85:e00407-19. <https://doi.org/10.1128/AEM.00407-19>.

**Editor** Charles M. Dozois, INRS—Institut Armand-Frappier

**Copyright** © 2019 American Society for Microbiology. All Rights Reserved.

Address correspondence to Guilian Yang, yangguilian@jlau.edu.cn, or Chunfeng Wang, wangchunfeng@jlau.edu.cn.

**Received** 19 February 2019

**Accepted** 29 April 2019

**Accepted manuscript posted online** 3 May 2019

**Published** 1 July 2019

and newly designed genetically engineered vaccines, such as virus-like particles (VLPs) (4), subunit vaccines (5), DNA vaccines (6), and reverse genetics-based vaccines (3). Since the first description of the immunogenic property of plasmid DNA in 1990, it has been used extensively to develop DNA vaccines against various pathogens, such as influenza virus (7, 8), NDV (9), and Zika virus (10, 11) and cancer (12) and HIV (13). Although the naked DNA vaccine possesses a number of advantages, such as tolerance to preexisting antibodies, there remain a number of drawbacks to the application of DNA vaccines in the field. One of the major problems is the immunization route, which is dependent on intramuscular or intradermal injection together with electroporation by a gene gun, limiting the application of these vaccines in the field due to inconvenience, especially for animal production. For such cases, bacterial vector DNA vaccine delivery systems, such as recombinant attenuated *Salmonella* vector (RASV), have received increasing attention due to the associated convenience of amplification and administration. In particular, the regulated-delayed-lysis *Salmonella* strain, which has been genetically engineered to lyse gradually *in vivo* after immunization, provides an attractive DNA vaccine delivery platform without an antibiotic selection marker (7). *Salmonella* lysis is based on the *asd* and *murA* genes, which are responsible for complete bacterial cell wall synthesis. The absence of both genes could result in *Salmonella* lysis. In the construct, the production of both Asd and MurA is dependent on the arabinose-controlled *araC* P<sub>BAD</sub> promoter located in the plasmid. After immunization, the absence of arabinose *in vivo* results in a gradual decrease in the production of Asd and MurA, which in turn leads to gradual *Salmonella* lysis *in vivo* (14).

Another important factor affecting the immunity of the exogenous antigen of the DNA vaccine is plasmid size as a large plasmid could decrease the efficiency of plasmid translocation from the cytoplasm to the nucleus, where transcription occurs. To overcome this disadvantage, a newly defined minicircle DNA (mcDNA) containing only the eukaryotic promoter and gene of interest (15) has attracted attention. The parental plasmid could be transformed into mcDNA and a miniplasmid by site-specific recombinases such as the Cre recombinase (16), ParA resolvase (17), and C31 integrase (18). Cre recombinase is a 38-kDa tyrosine recombinase enzyme derived from the P1 bacteriophage with 343 amino acids and recognizes a portion of the specific 34-bp DNA sequence (*loxP*) and deletes the DNA sequence between two *loxP* sites (19). The Cre-*loxP* system has been employed extensively in genetic engineering (20, 21) as well as mcDNA production (16). Notably, there are also some other similar *loxP*-like sites that could be recognized by Cre recombinase, such as the *lox66/lox71* (22) sites and *loxS1/loxS2* sites (23).

Because it is much smaller than the parental plasmid, mcDNA could dramatically increase the efficiency of translocation into the nucleus, which could therefore result in high expression levels. In addition, the removal of all bacterial sequences from the plasmid vector, including any antibiotic resistance genes, makes mcDNA a safer alternative than plasmids. The administration of mcDNA also provided prolonged transgene expression *in vivo* (24), enhanced serum stability (25) and increased resistance to shearing forces (26). Since its discovery, mcDNA has been used mainly in the field of gene therapy for human use. Most recently, the application of mcDNA as a vaccine delivery tool began in 2013 (27), and it appeared to induce a significantly stronger immune response than the parental plasmids (25, 28), especially in terms of the CD8<sup>+</sup> T cell-mediated cellular immune response (27). However, the application of mcDNA in vaccine studies has mainly focused on human diseases, such as cancer (29–31) and hepatitis B virus (HBV) (32) and HIV (33) infections, probably due to the complicated purification process, low production rate, and high preparation cost of mcDNA, which dramatically restrict the application of this system in practical veterinary applications. To date, there is no report on the application of mcDNA technology in veterinary vaccine studies. Therefore, the idea of using RASV to deliver mcDNA vaccines for veterinary application has elicited our interest recently. If successful, this mcDNA delivery system will provide a novel platform for veterinary vaccine application.

One of the key factors necessary to obtain high-purity mcDNA is the strict control of

recombinase expression *in vitro*. The plasmid harboring recombinant sites needs to be present at high copy numbers before recombination occurs, implying that recombinase must be completely absent. On the other hand, when required, the synthesized recombinase should efficiently target the recombinant sites, leading to high yields of mcDNA. To achieve this goal, some inducible promoters, such as the arabinose-dependent *araC* P<sub>BAD</sub> promoter (18) and temperature-sensitive cI857/PR promoter (15), have been used previously for efficient production of mcDNA *in vitro*. Another approach for regulated synthesis of recombinase usually relies on *in vivo* promoters such as the cytomegalovirus (CMV) promoter (34–36) and phosphoglycerate kinase (PGK) promoter (37). Different transcription and translation efficiencies for the CMV and PGK promoters have been previously reported because the CMV promoter could also significantly initiate gene transcription in *Escherichia coli* strains (38), which compromises the application of this promoter for our purpose, i.e., for strict control of the expression of recombinase *in vitro*. In contrast, the strict repression of the activity of the PGK promoter in the *E. coli* strain makes this promoter a suitable tool for our purpose.

In this study, we built up a novel Cre recombinase-mediated *in vivo* mcDNA (CRIM) platform for the production of mcDNA *in vivo* based on the presence of Cre recombinase driven by the PGK promoter. The plasmid could replicate as a complete parental plasmid *in vitro* and then transform into mcDNA *in vivo* by itself. Then, we used this CRIM platform to express the HN gene of genotype VII NDV and evaluated the protective effects of the mcDNA when delivered by regulated-delayed-lysis *Salmonella*. The results showed that CRIM-HN significantly improved the host immune response and provided efficient protection against wild-type NDV challenge, which provides a novel option for poultry vaccine development.

## RESULTS

**Construction of a eukaryotic expression vector harboring both *lox66/lox71* recombination sites and the PGK-Cre cassette.** The eukaryotic expression vector pYA4545 has been demonstrated to be an effective antigen delivery vector in recombinant *Salmonella* vaccines (7). To further extend the application of this vector, we first introduced *lox66/lox71* sites outside the CMV-EGFP-SV40-poly(A) cassette (where EGFP is enhanced green fluorescent protein and SV40 is simian virus 40) in the plasmid pYA4685, yielding pYL19 (Fig. 1A). Then, the PGK-Cre-poly(A) cassette was introduced into pYL19 to construct pYL46 (Fig. 1B), which would express Cre recombinase from the PGK promoter once the plasmid entered the cell nucleus. The principle underlying this novel platform is indicated in Fig. 1C; once pYL46 enters the nucleus after transfection or is delivered by bacteria to host cells (*in vivo*, early), the transcribed mRNA of Cre recombinase from the PGK promoter is transferred to the cytoplasm, followed by transcription to Cre recombinase. The synthesized Cre could then mediate the recombination between the *lox66* and *lox71* sites located in other pYL46 plasmids that were had not yet been translocated into the nucleus, resulting in the formation of mcDNA harboring EGFP or other genes of interest (GOIs), as well as MP plasmids (*in vivo*, middle). Therefore, the newly released mcDNA could be transferred into the nucleus with ease since it is smaller than the parent plasmid (1,888 bp versus 9,668 bp), resulting in increased efficiency of transcription and translocation (*in vivo*, late).

**PGK promoter-derived Cre recombinase transformed plasmid into mcDNA in 293T cells.** To determine whether Cre recombinase could be produced from the PGK promoter in pYL46, the plasmid was transfected into 293T cells, and the total proteins were isolated at 24 h posttransfection and subjected to Western blotting using a Cre-specific antibody as the primary antibody. The results showed that Cre recombinase was successfully synthesized in cells transfected with pYL46, while no Cre production was detected in either empty 293T cells or cells transfected with pYL19 (Fig. 2A). In addition, the presence of Cre recombinase was also confirmed by indirect immunofluorescence (IIF) analysis, in which red fluorescence indicated the presence of Cre in the pYL46 group (Fig. 2B).

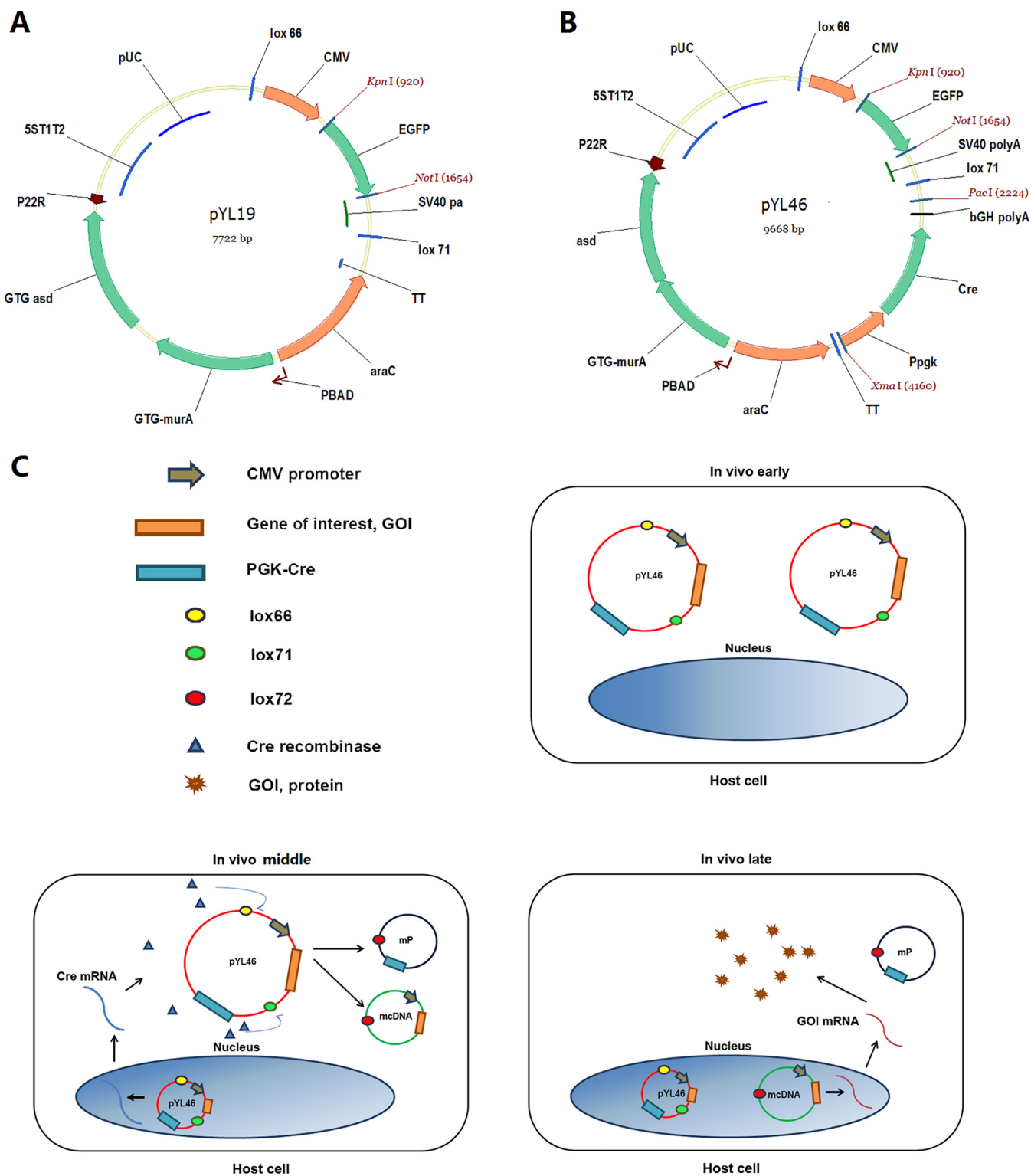


**FIG 1** Principle of Cre recombinase-mediated *in vivo* minicircle DNA (CRIM) platform. (A) The eukaryotic expression vector pYA4545 was used as the template to insert *lox66* and *lox71* sites, yielding pYL19. (B) The PGK-Cre cassette was inserted into pYL19, yielding pYL46, which contained a Cre recombinase expression cassette and *lox66/lox71* recombination sites. (C) The principle of CRIM technology is as follows: (i) at the stage *in vivo* early, the transfected pYL46 plasmids are maintained as a complete parental plasmid; (ii) at the stage *in vivo* middle, some of the parental plasmids translocate into the nucleus and are transcribed, leading to the cytoplasmic synthesis of Cre recombinase, which mediates recombination between the *lox66* and *lox71* sites to produce mcDNA; (iii) at the stage *in vivo* late, the smaller, newly formed mcDNA is translocated into the nucleus more efficiently than the parental plasmid, leading to enhanced transcription of the gene of interest (GOI).

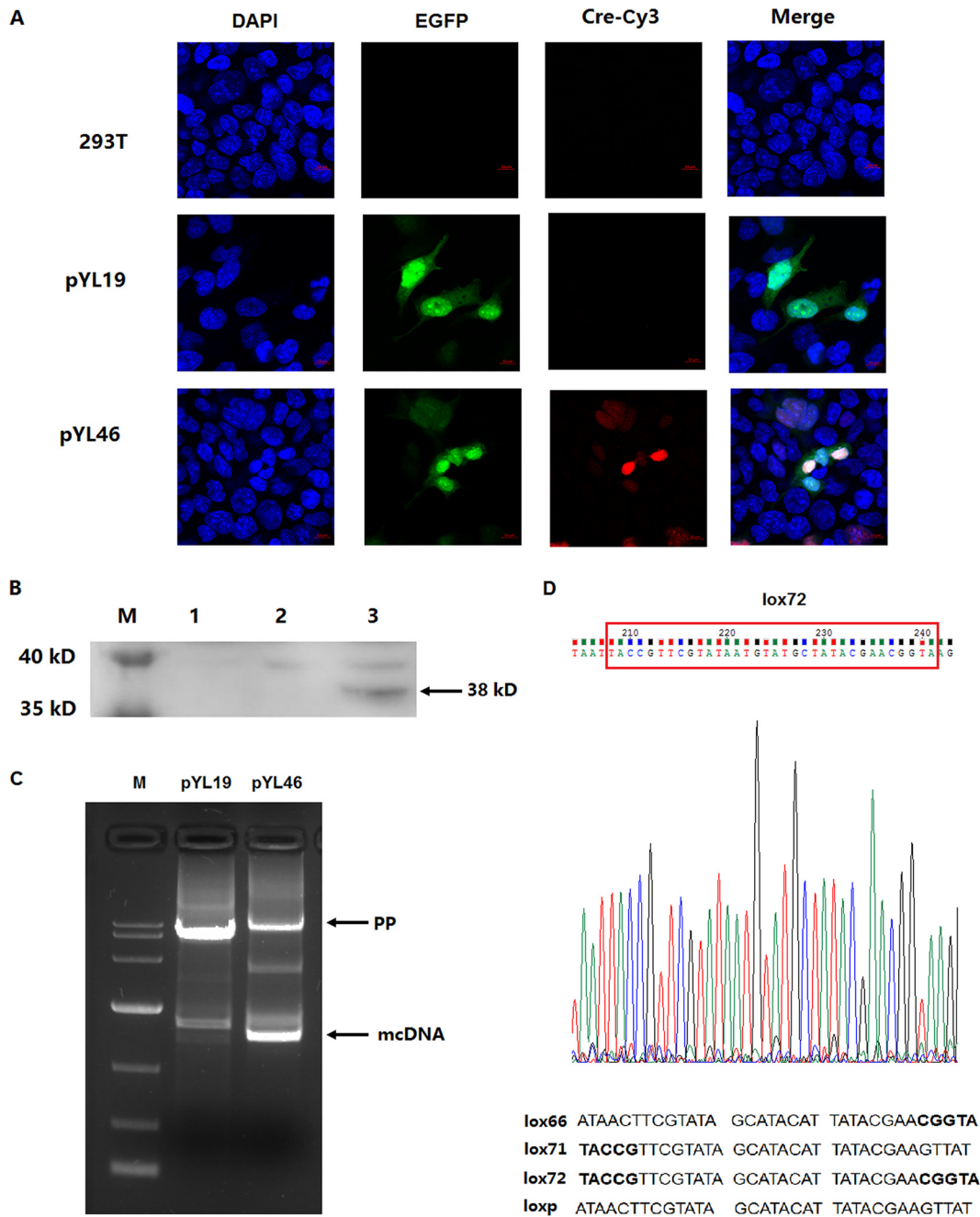


**FIG 2** Production of mcDNA by Cre recombinase under the PGK promoter. The parental plasmid (PP) pYL46 was transfected to 293T cells, and the total proteins were collected at 24 h posttransfection. The presence of Cre recombinase was confirmed by both indirect immunofluorescence (A) and Western blotting (B). Blue, 4',6'-diamidino-2-phenylindole (DAPI)-labeled nucleus; green, EGFP; red, Cre recombinase. Lane M, molecular size marker. (C) To confirm the presence of mcDNA, the cellular plasmids were extracted from 293T cells at 24 h posttransfection and subjected to PCR using the primer pair CMV-F1/CMV-R1. The PCR results indicated the formation of mcDNA in pYL46-transfected cells. (D) Recombination between the *lox66* and *lox71* sites, yielding *lox72*, was confirmed by DNA sequence analysis as indicated.

To evaluate whether the parental plasmid pYL46 could be transformed into mcDNA after transfection, the plasmids were extracted from 293T cells at 24 h posttransfection. The attempt to identify mcDNA directly from gel separation failed, probably due to the low concentration of extracted mcDNA. Therefore, we designed a pair of primers (CMV-F1/R1) that were located in the CMV promoter region and could simultaneously amplify both the mcDNA and parental plasmid. As expected, a clear PCR fragment of approximately 1,800 bp was observed in the extract from pYL46-transfected cells

(Fig. 2C), indicating the production of mcDNA in 293T cells. Additionally, there remained a large PCR product corresponding to the size of the pYL46 plasmid (Fig. 2C), which was not unexpected, as a number of pYL46 plasmids had not yet been transformed to mcDNA. In other words, the extracts from pYL46-transfected cells contained a mixture of parental plasmid and mcDNA. The purified PCR band was also sequenced to confirm the presence of *lox72* (Fig. 2D), indicating the occurrence of recombination between the *lox66* and *lox71* sites.

**Increased nuclear entry of plasmid DNA and production of EGFP in pYL46-transfected cells.** To determine whether the formation of mcDNA could increase nuclear entry, the DNA components of the cell nuclei were collected 24 h posttransfection. As expected, the PCR results demonstrated the presence of both mcDNA and parental plasmid in the nuclei of pYL46-transfected cells, whereas only the complete plasmid could be detected in the pYL19 group (Fig. 3A), indicating that the mixture of mcDNA and parental plasmid could translocate into the nucleus simultaneously. Consistent with previous results (Fig. 2C), a much weaker band corresponding to the size of pYL46 was also observed in the nucleus. Real-time PCR was then used to evaluate the number of plasmid copies in the cell nuclei in both groups. The results showed that mcDNA production dramatically increased the levels of EGFP/glyceraldehyde-3-phosphate dehydrogenase (GAPDH) in the pYL46 group (Fig. 3B), indicating that the small mcDNA could enter the nucleus more efficiently than the parental plasmid, which is consistent with a previous report in which small plasmids increased uptake efficiency in a 2-fold range compared with that of large plasmids (39).

Then, quantitative reverse transcription-PCR (qRT-PCR) and Western blotting were performed to further determine the levels of transcribed mRNA and translated protein after plasmid translocation. The qRT-PCR results showed that the mRNA levels of EGFP in pYL46-transfected cells increased steadily from 12 h to 48 h and were approximately 2- to 3-fold higher than those in cells transfected with pYL19 at 24 h and 48 h (Fig. 3C). Consistent with these results, EGFP production at both 24 h and 48 h increased substantially, especially at 24 h, exhibiting an approximately 2-fold increase in yield compared with that of the pYL19 group (Fig. 3D and E). In conclusion, mcDNA production in cells transfected with pYL46 significantly increased the nuclear entry of DNA, mRNA transcription, and protein translation, which was ideal for stimulation of the systemic immune response.

**Increased production of EGFP by pYL46 delivered by *Salmonella* in chickens.** To further determine whether the increased production of EGFP by pYL46 could be observed *in vivo*, chickens were orally inoculated with the *Salmonella* strain  $\chi$ 11218 harboring pYA4545, pYL19, or pYL46, and liver samples were collected at day 7 postinoculation and subjected to *in vivo* imaging. Compared with levels in livers from the  $\chi$ 11218(pYA4545) group (Fig. 4A and B and C) and  $\chi$ 11218(pYL19) group (Fig. 4D and E and F, left), a distinct increase in fluorescence intensity was observed in the  $\chi$ 11218(pYL46) group (Fig. 4D and E and F, right). The average fluorescence intensity in the  $\chi$ 11218(pYL46) group was approximately  $8.05 \times 10^9$ , which was significantly higher than  $4.95 \times 10^9$  ( $P < 0.05$ ) and  $3.93 \times 10^9$  ( $P < 0.01$ ), in the livers of the  $\chi$ 11218 (pYL19) and  $\chi$ 11218 (pYA4545) groups (Fig. 4G). The mRNA levels of EGFP in the chicken livers were then analyzed by qRT-PCR (Fig. 4H), and the results showed that the EGFP/chicken GAPDH (cGAPDH) ratio in the  $\chi$ 11218(pYL46) group was significantly higher than that in the  $\chi$ 11218(pYL19) group (mean value, 18.7 versus 7.42) ( $P < 0.001$ ) (Fig. 4I). All of the results above demonstrated that the *Salmonella* strain could deliver the EGFP gene cassette into chickens more efficiently with our CRIM vector than with a conventional plasmid.

**Construction of the HN expression plasmid.** Then, pYL19 and pYL46 were used to construct the HN expression plasmid pYL43 (Fig. 5A) and minicircle DNA parental plasmid pYL47, respectively (Fig. 5B). To detect the synthesis of the HN gene, purified plasmids with similar colony numbers were transfected into 293T cells and subjected to the IIF assay at 24 h posttransfection. Compared with cells transfected with the empty

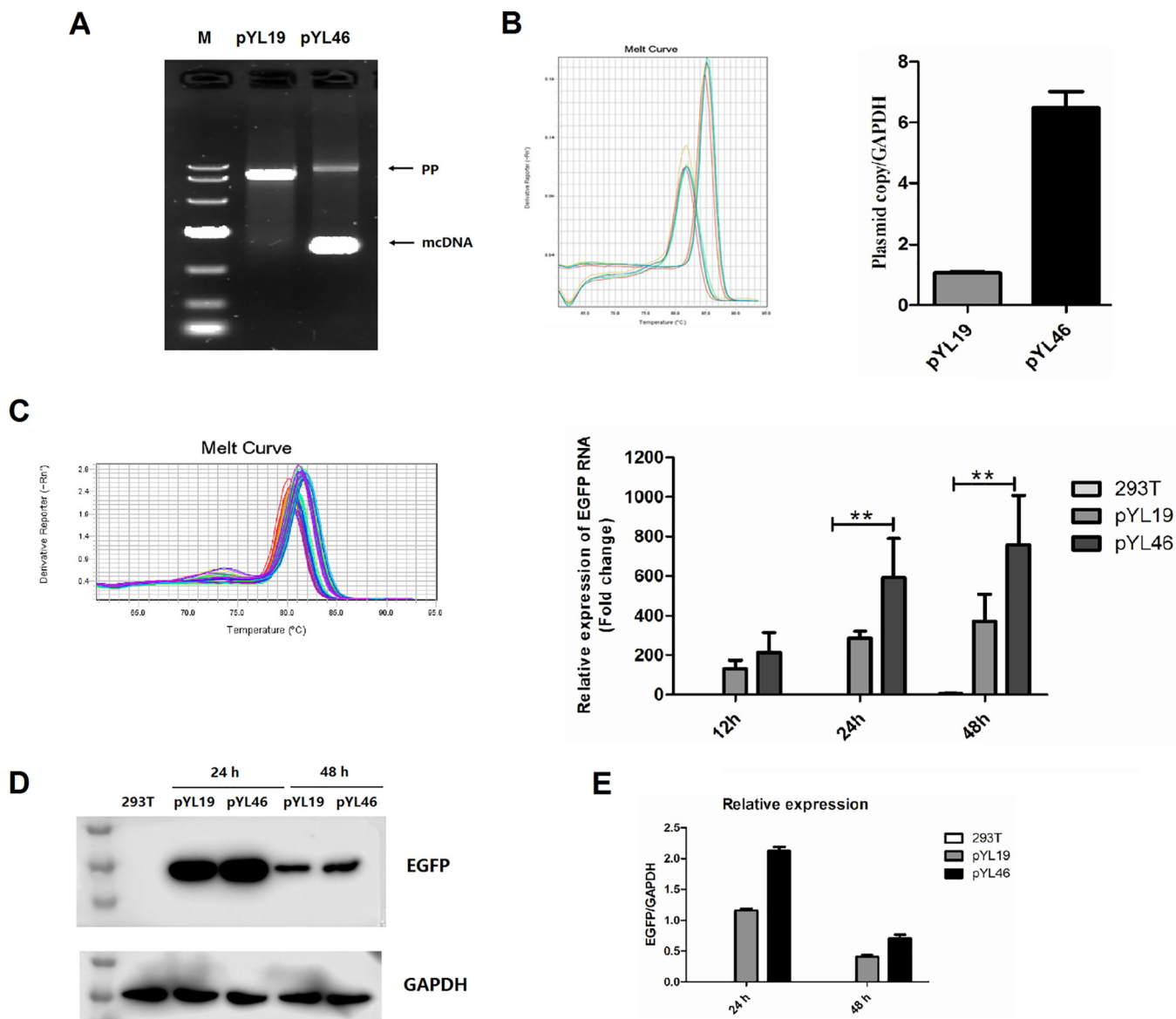


**FIG 3** Formation of mcDNA increased the nuclear entrance of mcDNA, the transcription of mRNA, and translation of protein. (A) The total DNA components were isolated from the nuclei of 293T cells transfected with pYL19 or pYL46 at 24 h posttransfection and subjected to PCR using primers CMV-F1/CMV-R1. The results confirmed the presence of mcDNA and parental plasmid pYL46 in the nucleus. Lane M, molecular marker; PP, parental plasmid. (B) Total DNA was further analyzed by real-time PCR, and the relative quantities of plasmid copy/GAPDH were determined. (C) The mRNAs were collected at 12 h, 24 h, and 48 h posttransfection from cells transfected with pYL19 and pYL46, and analyzed by qRT-PCR, and the relative expression levels of EGFP mRNA were calculated using mRNA of GAPDH as a control. (D) Total protein was collected at 24 h and 48 h and analyzed by Western blotting. (E) Relative band intensities of EGFP/GAPDH were calculated by ImageJ software. The results are represented as means  $\pm$  SEM ( $n = 3$ ), and statistical significance was calculated by one-way ANOVA and a Tukey posttest. \*\*,  $P < 0.01$ .

vector pYA4545, distinct green fluorescence was observed in cells transfected with both pYL43 and pYL47 (Fig. 5C). In particular, the production of Cre recombinase in pYL47-transfected cells was also observed (Cy3 labeled; red fluorescence), as expected (Fig. 5C, indicated by arrows).

**Increased production of serum IL-4 in both experiments.** The concentrations of both interleukin-4 (IL-4) and gamma interferon (IFN- $\gamma$ ) in serum collected from chickens at 49 days postvaccination (dpv) were determined by enzyme-linked immunosorbent assay (ELISA) kits. The results showed that the production levels of IFN- $\gamma$  were not significantly different in experiments 1 and 2 (Exp1 and Exp2, respectively), except for the those of the vaccine group in Exp1 (Fig. 6A and C). On the other hand, the production of IL-4 in Exp1 showed that chickens immunized with pYL47 induced

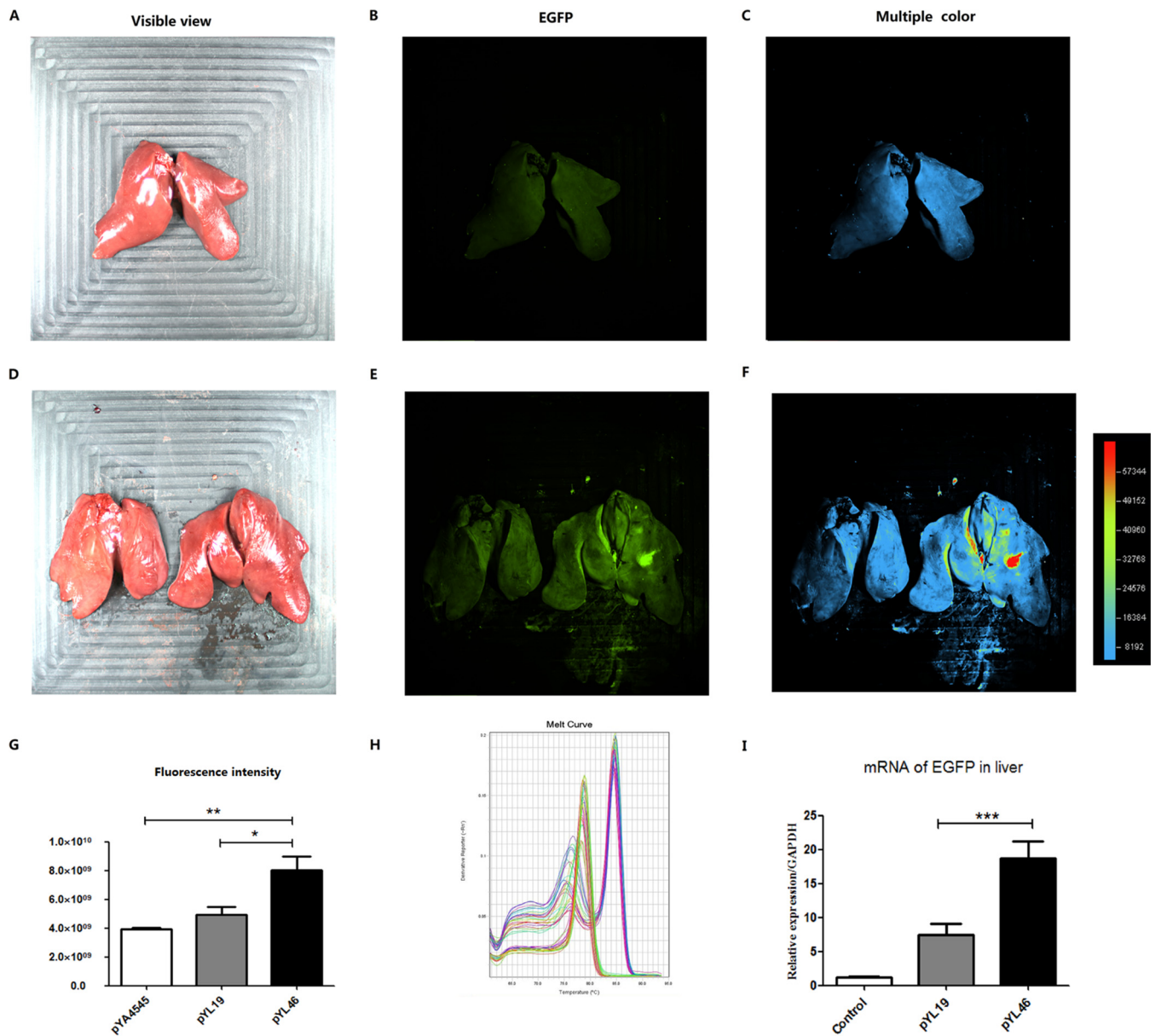


**FIG 4** Increased delivery of EGFP to chicken livers by *Salmonella* harboring pYL46. Chickens were orally inoculated with  $1 \times 10^9$  CFU of recombinant *Salmonella*  $\chi$ 11218 carrying pYA4545, pYL19, or pYL46. The livers were collected at day 7 postinoculation from chickens immunized with  $\chi$ 11218(pYA4545) (A, B, and C),  $\chi$ 11218(pYL19) (D, E, and F, left), and  $\chi$ 11218(pYL46) (D, E, and F, right). Data were analyzed by an *in vivo* imaging system (Vilber), including the visible view, EGFP view, and multicolor view, as indicated. (G) Fluorescence intensities were calculated, and the results are represented as means  $\pm$  SEM ( $n = 3$ ). (H and I) The liver samples were further analyzed by qRT-PCR targeting EGFP and chicken GAPDH (cGAPDH) genes. The relative abundances of the two mRNAs were calculated as EGFP/cGAPDH, and results are represented as means  $\pm$  SEM ( $n = 3$ ). Statistical significance was calculated by one-way ANOVA and a Tukey posttest. \*,  $P < 0.05$ ; \*\*,  $P < 0.01$ ; \*\*\*,  $P < 0.001$ .

significantly higher levels of IL-4 than those immunized with pYL43 ( $P < 0.01$ ) (mean value, 128.92 versus 104.62 pg/ml) (Fig. 6B). In Exp2, although the levels of IL-4 in both the pYL43 and pYL47 groups showed increasing trends compared with those in the saline and empty vector pYA4545 groups, no significant differences were observed (Fig. 6D).

**Increased production of the HI and ELISA antibodies by pYL47.** The hemagglutination inhibition (HI) antibody titers from immunized chickens were determined at 2-week intervals. The results showed that at 35 dpv in Exp1, only the inactivated NDV vaccine stimulated approximately 3 log<sub>2</sub> titers of HI antibody. At 49 dpv, the HI titer count was approximately 7 log<sub>2</sub> in the inactivated vaccine group, whereas approxi-

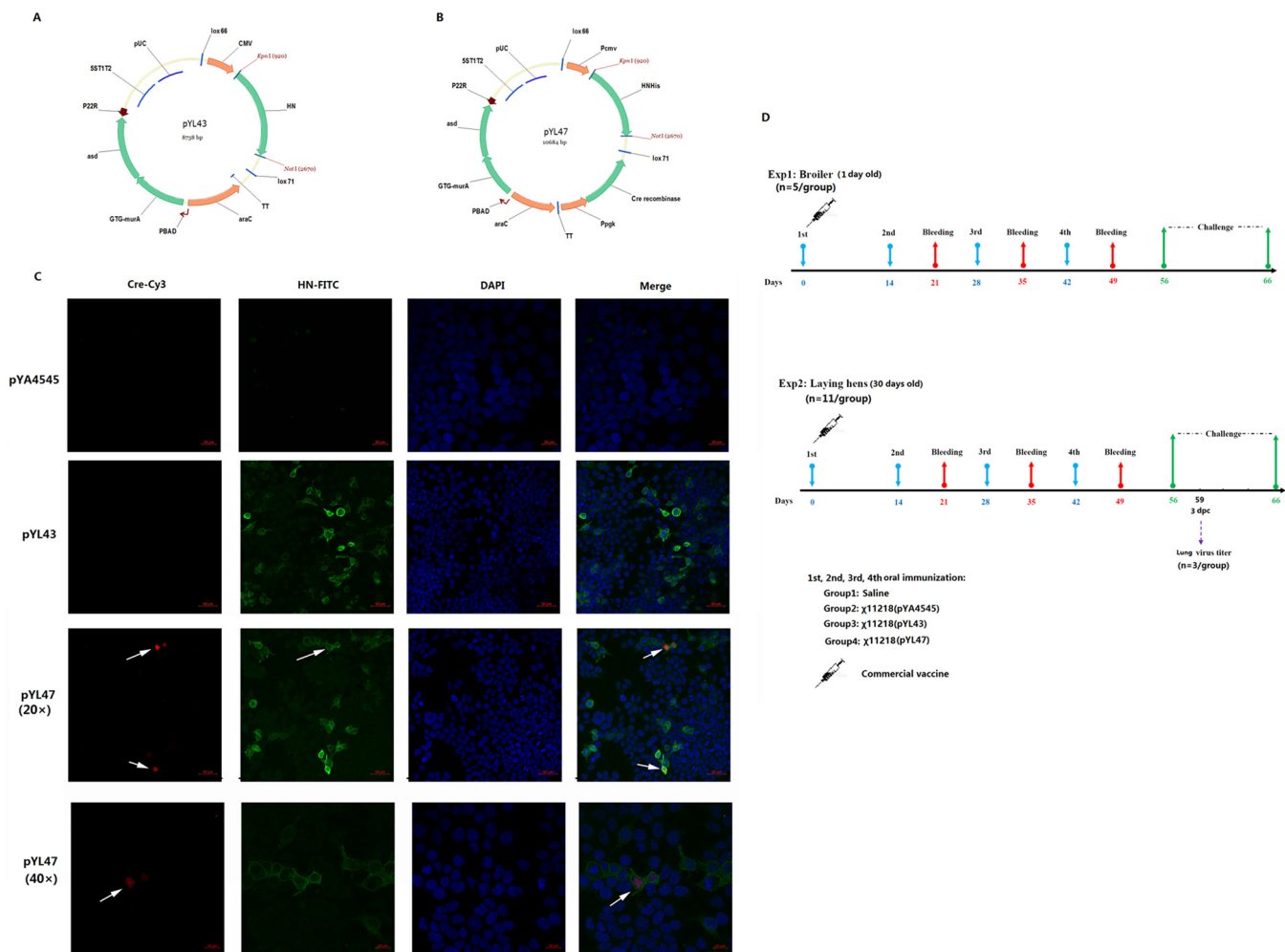


**FIG 5** Construction of a CRIM plasmid expressing HN protein of NDV and animal study protocol. (A and B) The His-tagged HN protein of genotype VII NDV was amplified and inserted into pYL19 and pYL46, yielding pYL43 and pYL47, respectively. 293T cells were transfected with pYL43 or pYL47. (C) At 24 h posttransfection, the cells were examined by indirect immunofluorescence, as described in Materials and Methods, to determine the production of HN (green) and Cre recombinase (red). Blue, 4',6'-diamidino-2-phenylindole (DAPI); green, FITC-labeled secondary antibody; red, Cy3-labeled secondary antibody. Arrows indicate the production of both HN and Cre recombinase in pYL47-transfected cells. (D) The animal study was performed twice, using broilers (Exp1) and laying hens (Exp2) as the animal models.

mately 3 log<sub>2</sub> antibody titers were observed in both pYL43- and pYL47-immunized chickens (Fig. 7A), indicating that the *Salmonella*-delivered DNA vaccine was not as efficient as the inactivated vaccine in terms of stimulation of the humoral immune response. A similar trend of HI antibody production was also observed in Exp2 (Fig. 7B), whereas low levels of the HI antibody were detected at 35 dpv, with approximately 2 log<sub>2</sub> titers in both the pYL43 and pYL47 groups. Approximately 3 log<sub>2</sub> antibody titers were observed at 49 dpv. Notably, although there was no statistically significant difference, there was consistently a slight increase in the production of HI antibodies in the pYL47 group compared with that of the pYL43 group in both Exp1 and Exp2, with a difference of approximately 1 log<sub>2</sub> in HI antibody titer (Fig. 7A and B). Serum NDV-specific antibodies were also detected by commercial ELISA kits. In Exp1, significantly increased production of NDV-specific serum IgG in chickens immunized with pYL47 was observed compared with the level in the pYL43 group (*P* < 0.05) (Fig. 7C), with an average antibody concentration of 274.98 pg/ml. A similar trend was also observed in Exp2, in which pYL47 immunization resulted in approximately 126.12 pg/ml NDV-specific IgG, even though no significant difference was observed (Fig. 7D).

**The CRIM plasmid pYL47 increased the survival rate after challenge.** In Exp1, all the chickens in the empty vector and saline groups appeared to be infected at day 3

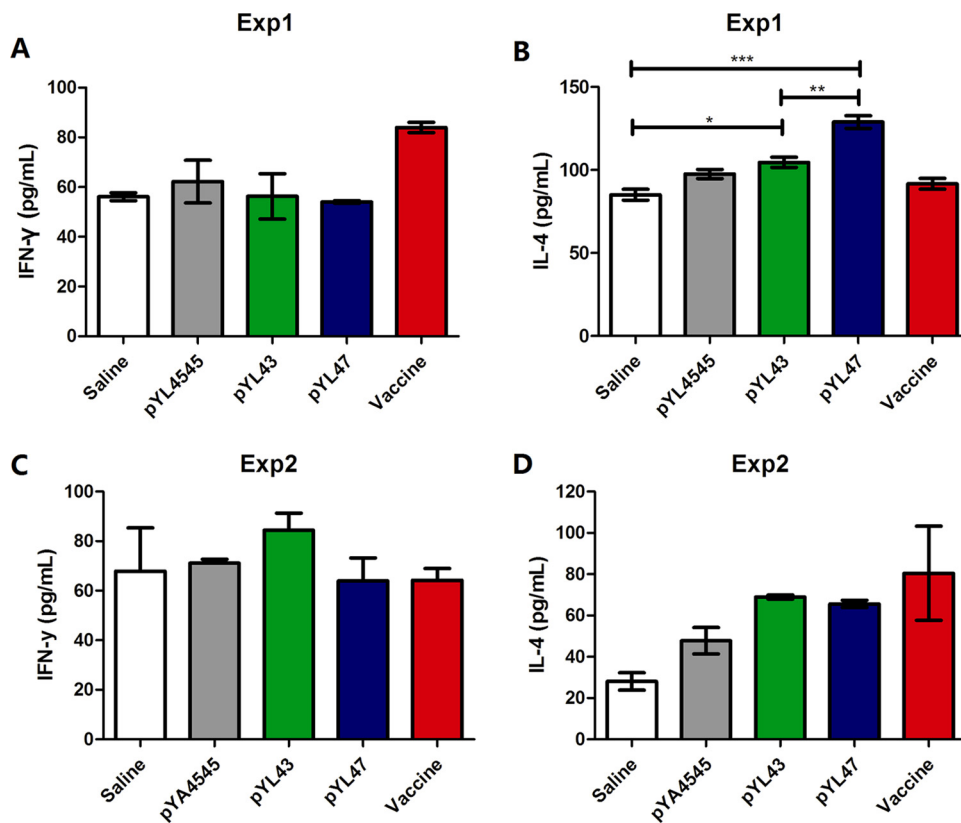


**FIG 6** Production of IL-4 and IFN- $\gamma$  in serum. The concentrations of serum IFN- $\gamma$  (A and C) and IL-4 (B and D) in Exp1 and Exp2 were determined by ELISA. The results are indicated as means  $\pm$  SEM ( $n = 3$ ). Statistical significance was calculated by one-way ANOVA and a Tukey posttest. \*,  $P < 0.05$ ; \*\*,  $P < 0.01$ ; \*\*\*,  $P < 0.001$ .

postchallenge (dpc), whereas a few chickens began to be infected at day 6 postchallenge among the pYL43- and pYL47-immunized chickens. The chickens started to die at day 6 postchallenge in the vector control group and saline group, and all the chickens died at days 8 and 9, respectively. The final protection rate in pYL43-immunized chickens was 40%, whereas the protection rate was 80% in the pYL47 group and 100% for the group treated with inactivated vaccine (Fig. 8A). In Exp2, chickens began to die at 5 or 6 dpc, and the final survival rates were 12.5%, 12.5%, 37.5%, and 50% for the saline, empty vector, pYL43, and pYL47 groups, respectively (Fig. 8B). The body weight changes in the animals in Exp2 showed that all the chickens began to lose weight at 4 dpc except those in the vaccine group. Compared with the saline and empty vector groups, pYL43-immunized chickens showed low body weight loss, whereas pYL47 immunization provided improved protection against weight loss (Fig. 8C).

**Decreased viral loads in the lungs of chicken challenged with pYL47.** The viral titers in the lungs were determined by viral dilution on DF-1 cells. The results showed that the titers were highest in groups that had not been vaccinated or had been vaccinated with the empty vector pYA4545, whereas the replication titers were very low in other groups and were similar in the groups immunized with pYL47 or the inactivated vaccine (Fig. 8D), especially for the pYL47 group, which showed significantly decreased titers compared with those of the empty vector group ( $P < 0.01$ ).

## DISCUSSION

In the present report, we describe the spontaneous transformation of a plasmid to mcDNA *in vivo*. The purpose of this study was to design a novel *in vivo* release platform for mcDNA production delivered by *Salmonella* for veterinary vaccine studies. For this purpose, the Cre recombinase has to be strictly repressed *in vitro* because any leaky

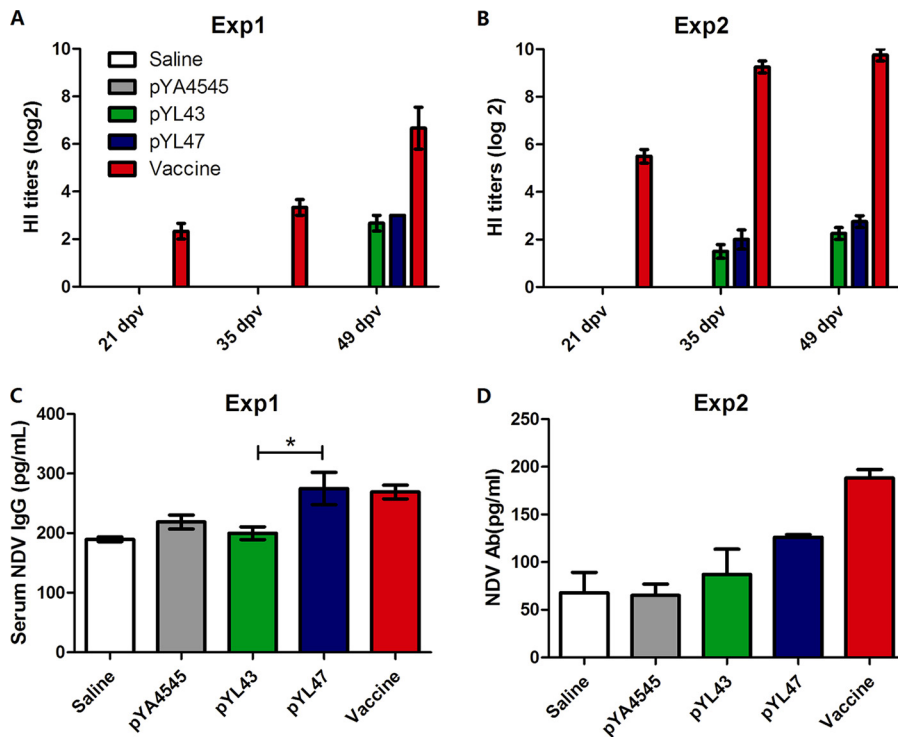


**FIG 7** Antibody response in both experiments. (A and B) The hemagglutination inhibition (HI) antibody titers in Exp1 and Exp2 were determined at days 21, 35, and 49 postvaccination (dpv). (C and D) The serum NDV-specific IgG antibodies at 49 dpv were also determined by ELISA in Exp1 and Exp2. The results are shown as means  $\pm$  SEM ( $n = 3$ ). Statistical significance was calculated by one-way ANOVA and a Tukey posttest. \*,  $P < 0.05$ .

production of Cre recombinase could result in undesired recombination between the *lox66* and *lox71* sites, yielding mcDNA *in vitro* that would be lost during bacterial cultivation due to the absence of a selective marker. In fact, we tried a number of regulated promoters to express Cre recombinase in *Salmonella*, including the *araC*-P<sub>BAD</sub> promoter (7), the PagC promoter for *in vivo* regulation (40), and the cI857/PR temperature-controlled promoter (41). Unfortunately, although all the mentioned promoters could dramatically decrease the production of Cre *in vitro*, there remained some leaky synthesis of Cre recombinase, resulting in the undesired presence of Cre, which in turn transformed the parental plasmid into mcDNA and a miniplasmid.

To achieve our goal, we then explored eukaryotic promoters, such as the CMV promoter and PGK promoter. According to a previous report, the PGK promoter had no activity in an *E. coli* strain, whereas the CMV promoter was a very strong promoter in *E. coli*. Using  $\beta$ -galactosidase ( $\beta$ -Gal) as a model, the strength of the PGK promoter-driven  $\beta$ -Gal activity was 37 in *E. coli*, which was significantly lower than the  $\beta$ -Gal activity observed under the CMV promoter, which was 10,600 (38). Therefore, we used the PGK-Cre-bpA plasmid to insert the PGK-Cre-poly(A) cassette into our construct, which finally exhibited absolutely no production of Cre recombinase *in vitro*, yielding the complete pYL46 parental plasmid harboring both the *lox66* and *lox71* sites and the Cre cassette.

The key feature of our novel technology is the transformation of the parental plasmid into mcDNA after transfection. Therefore, we attempted to extract mcDNA from 293T cells transfected with the parental plasmid pYL46. Unfortunately, all our attempts failed even though we tried different approaches, such as increasing the cell numbers and using different kits for purification of both genomic and plasmid DNA. However, we never achieved our goal by direct purification and DNA gel purification, probably due to the low mcDNA yield. Then, we designed a pair of primers located in

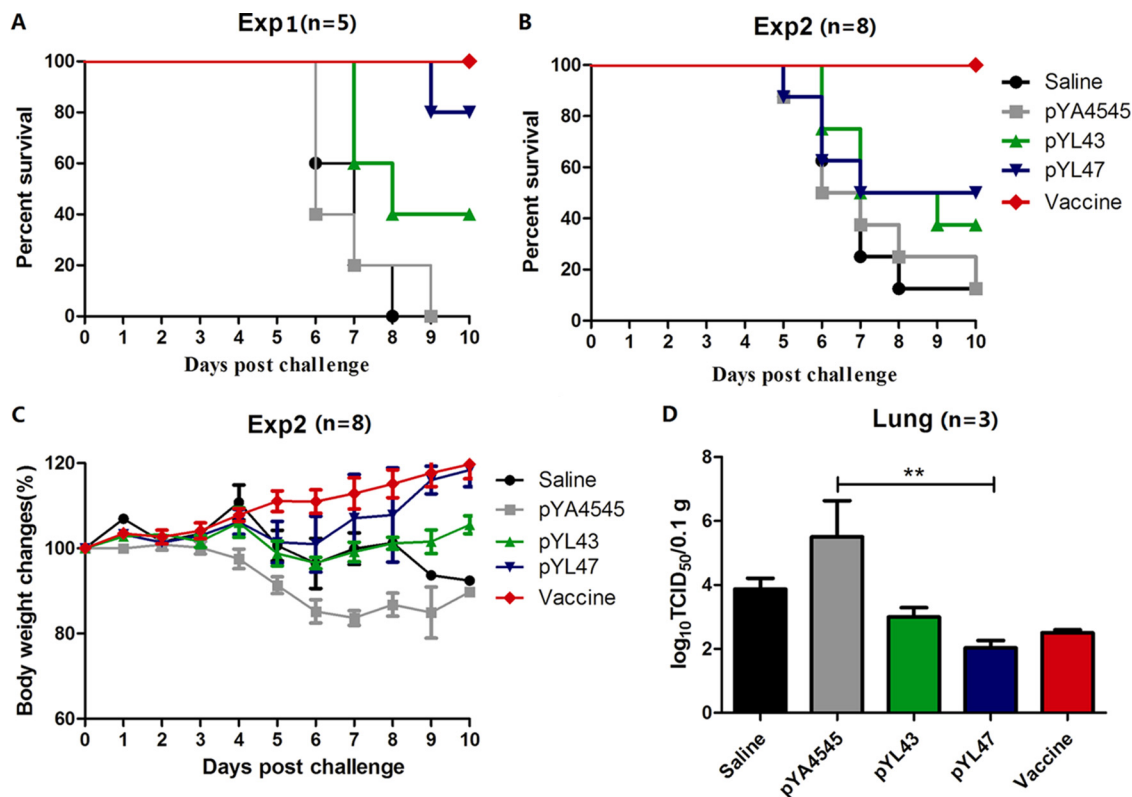


**FIG 8** Protection against NDV challenge with virulent NA-1 strain. (A and B) After challenge with  $10^6$  ELD<sub>50</sub> of NDV NA-1 strain, the chickens were observed for 10 days. Survival curves were calculated for Exp1 and Exp2. (C) Changes in body weight were also determined (Exp2). (D) At day 3 postchallenge, lung tissues were collected from each group ( $n = 3$ ), and the virus titers were determined by dilution on DF-1 cells. The results are expressed as means  $\pm$  SEM ( $n = 3$ ), and statistical significance was calculated by one-way ANOVA and a Tukey posttest (\*\*,  $P < 0.01$ ). TCID<sub>50</sub>, 50% tissue culture infective dose.

the CMV promoter region, and these primers were used to amplify both the complete parental plasmid and short mcDNA components. As expected, PCR products corresponding to the sizes of the parental plasmid and mcDNA were both detected by agarose gel electrophoresis (Fig. 2C and 3A), indicating successful production of mcDNA after transfection.

The regulated-delayed-lysis *Salmonella* strain has been engineered to lyse in the cytoplasm of host cells to release DNA vaccines more efficiently than traditional nonlysis *Salmonella* strains (7). In this study, the released plasmid DNA transformed to mcDNA and the miniplasmid after the synthesis of Cre recombinase, so, strictly speaking, our mcDNA vaccine was not a pure collection of mcDNA; instead, this vaccine included a mixture of mcDNA, the miniplasmid, and the residual parental plasmid. Thus, this system was different from previous mcDNA constructs for human application, which required complete absence of materials other than mcDNA. Our main purpose was to improve the immunological property of our veterinary vaccines, so a mixture of mcDNA could be acceptable in our study.

The poor immunogenicity of encoded antigens delivered by naked DNA vaccines has been noted previously (42). In both Exp1 and Exp2, the HI antibody titers increased much more slowly than those obtained with the inactivated vaccine (Fig. 7A and B), especially for the broiler chickens in Exp1, in which the HI antibody did not appear until 49 dpv. In fact, to further improve the efficiencies of the DNA vaccine, some studies used the DNA prime and protein boost strategy to achieve significantly increased antibody production (43, 44). Therefore, our next step could be the involvement of subunit vaccine in addition to our CRIM vaccine, which should be able to induce a better immune response than the DNA vaccine alone. The challenge study in Exp1 demonstrated that pYL47 could provide an 80% protection rate at day 10 postinfection.

**TABLE 1** Bacterial strains and plasmids used in this study

Strain or plasmid	Description	Source and/or reference
<b>Strains</b>		
$\chi$ 11218	<i>Salmonella</i> host strain for DNA vaccine study	Roy Curtiss III (7)
$\chi$ 6212	<i>E. coli</i> host strain for DNA cloning	Roy Curtiss III, University of Florida
<b>Plasmids</b>		
pYA4545	Eukaryotic expression vector in <i>Salmonella</i> , arabinose dependent	Roy Curtiss III (7)
pYA4685	pYA4545 expressing EGFP, eukaryotic expression vector in <i>Salmonella</i> , arabinose dependent	Roy Curtiss III (7)
pUC-HNopt	Codon-optimized HN gene of genotype VII NDV cloned in pUC57, Kan <sup>+</sup>	Genewiz, China
pYL19	pYA4685 harboring both <i>lox66</i> and <i>lox71</i> sites and MRS1/2 sites	This study
pYL46	pYL19 harboring PGK-Cre cassette	This study
pYL43	pYL19 harboring HN gene, expresses the HN under the CMV promoter	This study
pYL47	pYL46 harboring HN gene, expresses HN under the CMV promoter	This study

This result was actually rather impressive considering the relatively low HI antibody titers. It has been demonstrated that the mcDNA vaccine prefers to prime cytotoxic T-lymphocyte (CTL) responses and generate memory CD8 T-cell responses (27); therefore, one of the possible explanations for our results was that the CRIM vaccine could efficiently stimulate the cellular immune response in addition to the humoral immune response even though we did not evaluate this aspect in this study. In addition to the levels of the HI antibody, we also measured the serum levels of the NDV-specific IgG antibody using commercial kits. In general, the levels of NDV-specific IgG antibodies in pYL47-immunized chickens increased compared with the levels in the pYL43 group (Fig. 7C and D), indicating that some other antibodies could be responsible for the observed protection.

The survival rates for pYL47-immunized chickens differed between Exp1 and Exp2 (80% versus 50%, respectively). In fact, we noticed that there were some differences between broilers (Exp1) and laying hens (Exp2). We challenged the chickens in both studies with the same dose of virus ( $10^6$  50% embryo-lethal doses [ELD<sub>50</sub>]), but the broilers (Exp1) appeared to be more resistant to viral challenge than the laying hens (Exp2). One of the possible reasons underlying this effect was that the average body weights at the beginning of the challenge in Exp1 were approximately 2 kg, in contrast to 1.5 kg in Exp2. Other parameters were also observed to differ, such as the production of serum cytokines and ELISA antibodies, most likely due to differences in chicken species. For example, the inactivated vaccine resulted in dramatically increased production of IFN- $\gamma$  in broiler chickens in Exp1 (Fig. 5A), with no obvious simultaneous production of IL-4 (Fig. 5B). On the other hand, the CRIM vector pYL47 significantly stimulated the production of IL-4 but not IFN- $\gamma$  in Exp1 (Fig. 5A and B). However, the production trends for IL-4 and IFN- $\gamma$  in Exp2 were not similar to those in Exp1 (Fig. 5C and D). The increased production of IL-4 in pYL47-immunized broilers in Exp1 was possibly responsible for the relatively high titers of NDV-specific IgY antibodies (Fig. 7C).

In conclusion, we constructed a novel CRIM platform based on the PGK promoter and Cre recombinase. In combination with our previous regulated-delayed-lysis *Salmonella* vector, the novel CRIM vaccine provided significant protection against wild-type NDV challenge in a chicken model, indicating that our novel *Salmonella*-CRIM technology could provide a novel platform for poultry vaccine development.

## MATERIALS AND METHODS

**Bacterial strains and growth conditions.** The bacterial strains and plasmids used in this study are listed in Table 1. *Escherichia coli* (*E. coli*)  $\chi$ 6212 cells were used as the host strain during plasmid construction and grown in Luria-Bertani (LB) medium supplemented with 50  $\mu$ g/ml diaminopimelic acid (DAP) (Sigma) at 37°C with shaking. The *Salmonella*  $\chi$ 11218 strain was grown in LB medium supplemented with 0.1% arabinose (Sigma) and 50  $\mu$ g/ml DAP. When necessary, solid medium was prepared by addition of 1.5% (wt/vol) agar to the broth.

**DNA manipulation.** The primers used in this study are listed in Table 2. To construct a eukaryotic expression plasmid for minicircle DNA production, the *lox66/lox71* sites were introduced into pYA4685 by PCR as described later and were located outside the CMV promoter and SV40 poly(A) sequences. To

**TABLE 2** Primers used in this study<sup>a</sup>

Primers	Sequence
lox66-SacII-F	TATGCCCGGGTAAATACCGTTCGTATAATGTATGCTATACGAAGTTATGGGGTCATTAGGGGACTTTC
lox71-StuI-R	ACCAGGCCTTACCGTTCGTATAGCATACTATACGAAGTTATCCACCAGCATCCCCACATGCTTTG
4545-SacII-F	AATACCGCGGGTAATTGATTACTATTAATA
4545-StuI-R	GTAAGGCCTGCTCTATGGCTTCTACTG
PGK-F2-XmaI	TCCCCCGGGTCGAGGTCGACGGTATCG
PGK-R2-PaCI	CCTTAATTAACCAGCTGGTTCCTTCCTCAG
pYL19-F2-xmaI	TCCCCCGGGTGTGCCTGTCAAATGGACGAAG
pYL19-R2-PaCI	CCTTAATTAATTATGCATCGGGGAATTGCG
4545-StuI-F2	TATAGGCCTGGCGGGCTAGATCTTCCAAC
4545-SpeI-R2	ATTACTAGTCGCAATTCCTCCGATGCATAATG
MRS2-StuI-F	TATAGGCCTGGTCAAATGGGTATACC
MRS2-SpeI-R	ATTACTAGTCATATGTGGGCGTGAGGC
NA-HN-KpnI-F	ATAGGTACCAGGAGCCGCCACCATGGACA
NA-HN-NotI-R	GGAGCGCCGCTCAGTGGTGGTGGTGGTG CACTCTATCGTCTTCAGGA
CMV-F1	GTACGCCCTTATTGACG
CMV-R1	TTGGCATATGATACACTTG

<sup>a</sup>Underlined nucleotides are restriction sites; italicized nucleotides are the lox66/lox71 sites.

elaborate, the P<sub>CMV</sub>-EGFP-SV40 cassette was amplified using the primers lox66-SacII-F/lox71-StuI-R, whereas the vector fragment was amplified by the primers 4545-SacII-F/4545-StuI-R. The two PCR fragments were then digested with SacII/StuI and ligated, yielding pYL12. To further expand the application of our new plasmid, we also introduced two multimer resolution sites (MRS) into pYL12, which could be recognized by the recombinase ParA. A plasmid harboring MRS1 and -2 (MRS1/2) was synthesized by Genewiz (Suzhou, China); the MRS1 fragment was removed by XbaI/SacII digestion, and pYL12 was also digested with XbaI/SacII. The two fragments were then ligated to yield the pYL12-MRS1 plasmid. Then, the primers MRS2-stuI-F/MRS2-speI-R and 4545-stuI-F2/4545-speI-R2 were used to amplify the MRS2 fragment and the pYL12-MRS1 fragment individually. The two fragments were then digested with StuI/SpeI and ligated, yielding pYL19, which included both the lox66/lox71 sites and MRS1/2, although MRS1/2 were not associated with this study.

To introduce a Cre recombinase expression cassette under the PGK promoter into pYL12, the PGK-Cre-poly(A) gene was amplified using the primers PGK-F2-xmaI/PGK-R2-PaCI from the template plasmid pPGK-Cre-bpA (a gift from Klaus Rajewsky [plasmid 11543; Addgene]), whereas the pYL19 plasmid was used as a template to amplify vector sections using the primers pYL19-F2-xmaI/pYL19-R2-PaCI. After digestion with XmaI/PaCI, the fragments were ligated to yield pYL46. The HN gene of genotype VII of NDV was codon optimized for expression in chicken and cloned into the plasmid pUC-HNopt (Genewiz). The HN fragment was then amplified using the primers NA-HN-KpnI-F/NA-HN-NotI-R and double digested with KpnI/NotI. Then, the plasmids pYL19 and pYL46 were digested with the same enzymes and ligated with the HN fragments, yielding pYL43 and pYL47, respectively.

**Determination of Cre and EGFP expression in 293T cells by Western blotting and IIF.** To evaluate the synthesis of Cre recombinase and detect the recombination between lox66 and lox71 sites conducted by this recombinase, the plasmid pYL46 was purified by using a GoldHi EndoFree Plasmid Midi kit (Kangwei Co., China) and transfected into 293T cells using Lipofectamine 3000 (Life Technologies) according to the manufacturer's instructions. pYL19 was also included as a control with the same copy numbers. To elaborate,  $2 \times 10^6$  cells per well in six-well plates were transfected with 2  $\mu$ g of purified plasmid, and after 24 h and 48 h of incubation, whole-cell lysates were collected and subjected to SDS-PAGE and Western blotting using an anti-Cre antibody (GeneTex) and anti-EGFP antibody (BBI Life Science) as primary antibodies. After incubation with a horseradish peroxidase (HRP)-conjugated secondary antibody and probing with a substrate, specific bands were observed using an imaging system, and the relative levels were calculated using ImageJ software. The production of Cre recombinase was also determined by an indirect immunofluorescence (IIF) assay as described previously (45) in 24-well plates using the Cre antibody mentioned above as the primary antibody and Cy3-labeled goat anti-rabbit IgG(H+L) (Beyotime, China) as the secondary antibody. Fluorescence was observed under a confocal microscope (LSM710; Zeiss).

**Extraction of plasmid and mcDNA from transfected cells.** To determine whether the complete plasmid could be transformed to mcDNA after transfection, the plasmid DNA from 293T cells was extracted at 24 h posttransfection using a QIAprep Spin Plasmid kit (Qiagen) according to a previously described method (46). Then, the primers CMV-F1/CMV-R1 were used to amplify either the parental pYL46 plasmid or mcDNA, and the bands were then purified from the gel and sequenced to confirm recombination between the lox66 and lox71 sites, yielding a lox72 site.

**Quantification of plasmid DNA copies in the nucleus.** The cell nuclei were collected from 293T cells transfected with both the pYL19 and pYL46 plasmids at 12 h posttransfection by using a nuclear DNA extraction kit (BestBio, China). To remove the associated extranuclear plasmid DNA, the nuclei were pelleted, rinsed twice in stock nucleus isolation buffer without NP-40, and resuspended in 1 ml of stock nucleus isolation buffer with 1% paraformaldehyde (PFA) and without NP-40 (47). The nuclear DNA was then isolated according to a previously described method (48) with minor modifications. To elaborate, the isolated nuclei were incubated with lysis buffer consisting of 0.5% SDS, 100  $\mu$ g/ml proteinase K, and

**TABLE 3** Primers used in real-time PCR

Primer	Sequence	Product size (bp)
EGFP-F	CAGCCACAACGTCTATATCATGG	122
EGFP-R	GGGTGTTCTGCTGGTAGTGGT	
hGAPDH-F	GCACCGTCAAGGCTGAGAAC	138
hGAPDH-R	TGGTGAAGACGCCAGTGGA	
cGAPDH-F	CTCTGGCAAAGTCCAAGTGGTG	132
cGAPDH-R	GCCCTGAAGTGCCGTGTGTA	

20  $\mu$ g/ml DNase-free RNase overnight at 50°C. Then, the total DNA was purified with 1 volume of Tris-EDTA (TE)-saturated phenol (Life Technology, USA), followed by another extraction in one volume of phenol-chloroform-isoamyl alcohol (25:24:1). Total DNA was then precipitated with 2 volumes of 100% ethanol for 30 min at  $-20^{\circ}\text{C}$  and centrifuged at 12,000 rpm for 10 min at  $4^{\circ}\text{C}$ . After an additional two washes with 70% ethanol, the precipitated DNA was stored in double-distilled  $\text{H}_2\text{O}$  (dd $\text{H}_2\text{O}$ ) at  $-20^{\circ}\text{C}$  until further use. PCR was performed using the primers CMV-F1/R1 to confirm the presence of mcDNA in the nucleus, and then real-time PCR was performed to determine the relative plasmid (mcDNA) copy numbers. To elaborate, real-time PCR was performed in an ABI 7500 system (Applied Biosystems) in a 96-well plate. A 25- $\mu$ l reaction volume with 12.5  $\mu$ l of SYBR green stain (FastStart Universal SYBR green Master; Roche), 10 ng of template DNA, and 0.2 mM each primer pair (CMV-F1/CMV-R1 or GAPDH-F/GAPDH-R) (Table 2) were used for the reactions, targeting the CMV promoter regions of both the parental plasmid and mcDNA or the GAPDH gene of 293T cells, respectively.

**Determination of the number of transcribed mRNA copies of EGFP by real-time qRT-PCR.** To further determine the efficiency of transcription, total RNA was isolated from transfected cells at 12, 24, and 48 h posttransfection using an RNA Extraction kit (TaKaRa) according to the manufacturer's instructions. One hundred nanograms of total RNA from each sample was then reverse transcribed to cDNA using a reverse transcription system (TaKaRa) according to the manufacturer's instructions. At the end of the procedure, cDNA was diluted to a concentration of 10 ng/ $\mu$ l. The nucleotide sequences of the primers are shown in Table 3. Quantitative reverse transcription-PCR (qRT-PCR) was performed in an ABI 7500 system (Applied Biosystems) in a 96-well plate. A 25- $\mu$ l reaction volume with 12.5  $\mu$ l of SYBR green stain (FastStart Universal SYBR green Master; Roche), 10 ng of cDNA as the template, and 0.2 mM each primer pair (EGFP-F/EGFP-R or hGAPDH-F/hGAPDH-R) were used for the reactions targeting the EGFP gene and human GAPDH gene of 293T cells, respectively ( $n = 3$ ).

**Synthesis of EGFP *in vivo* by pYL19 and pYL46 delivered by the *Salmonella* vector.** To determine whether our novel CRIM platform works *in vivo*, we first transformed both the pYL19 and pYL46 plasmids into competent  $\chi$ 11218 cells as described previously (49). Thirty-day-old laying hens (local farm) were orally inoculated with approximately  $1 \times 10^9$  CFU of  $\chi$ 11218 harboring the empty vector pYA4545, pYL19, or pYL46 in 100  $\mu$ l of saline, with three birds per group. At day 7 postinoculation, all the chickens were necropsied, and the livers were collected and subjected to *in vivo* imaging (Vilber); then, the fluorescence intensities of the synthesized EGFP were determined. In addition, the total RNA samples from the individual livers were collected by using an RNA Extraction kit (TaKaRa) and analyzed by qRT-PCR as described above using the primers EGFP-F/EGFP-R and cGAPDH-F/cGAPDH-R (Table 3) for amplification of the EGFP and chicken GAPDH (cGAPDH) genes, respectively; the results are presented as mRNA levels of EGFP/cGAPDH ( $n = 3$ ). All experimental procedures and animal management procedures complied with the requirements of the Animal Care and Ethics Committees of Jilin Agriculture University, China.

**Synthesized HN and Cre recombinase in 293T cells.** The plasmids pYL43 and pYL47 constructed previously were transfected into HEK293T cells with the same copy numbers using Lipofectamine 3000 (Life Technologies) as described above. The empty vector pYA4545 was also included as a negative control. Synthesis of the HN proteins was determined by an IIF assay at 24 h posttransfection. A mouse anti-His monoclonal antibody (A02050; Abbkine) was used as the primary antibody at a dilution of 1:1,000 as recommended, followed by a fluorescein isothiocyanate (FITC)-labeled goat anti-mouse IgG antibody (Cwbiotech, Beijing, China). Simultaneously, the production of Cre recombinase in cells transfected with pYL47 was also determined by IIF as described above. The fluorescence was then detected by confocal microscopy (Zeiss, Germany).

**Animal study.** Two sets of chicken experiments were performed using broilers (1 day old) and laying hens (30 days old) (Hongda Animal Technology Co., Ltd., Changchun, China), for experiment one (Exp1) and experiment two (Exp2), respectively. The basic immunization and challenge protocols were the same for both experiments, except for a few differences regarding the number of chickens as well as the challenge study, as shown in Fig. 5D.

To elaborate, 1-day-old broiler chickens (Exp1) or 30-day-old laying hens (Exp1) were divided into separate isolators, with 5 chicks per group (Exp1) or 11 chicks per group (Exp2). The chickens in Exp2 were fed after arrival until day 30 to exclude the presence of parental hemagglutination inhibition (HI) antibody. All the birds were orally inoculated with approximately  $1 \times 10^9$  CFU of  $\chi$ 11218 harboring pYA4545, pYL43, or pYL47 individually as primary vaccinations (indicated as 0 dpv), and chickens inoculated with saline were also included as negative controls. In addition, chickens intramuscularly injected with commercial genotype VII NDV vaccine (Jiangsu Nannong Hi-Tech Co., Ltd, China), once at 0 dpv, according to the product instructions were included as positive controls. The chickens were then subjected to boosting an additional three times with recombinant strains at 14, 28, and 42 dpv, and

blood samples were collected at 21, 35, and 49 dpv. The HI antibody levels were determined using 1% chicken red blood cells (RBCs) with 4 hemagglutination (HA) units of the NDV-specific antigen (NA-1; Jilin University, China) per well as described previously (50). The serum NDV-specific IgG antibody levels and concentrations of IL-4 and IFN- $\gamma$  in the serum from 49 dpv were determined using a commercial ELISA kit according to the manufacturer's instructions (Kete, Inc., Jiangsu, China).

The chickens were then challenged with the genotype VII NDV wild-type strain NA-1 at a dose of  $10^6$  ELD<sub>50</sub> via nasal drops at 56 dpv, and the clinical signs and survival rates were observed and recorded over the next 10 days. For Exp2, viral replication in the lungs was also determined as described previously (51) with minor modifications. To elaborate, three chickens from each group were sacrificed on the 3rd dpc for quantification of challenge virus replication. Tissue samples, including lung, spleen, and bursa samples, were collected, homogenized in cell culture medium (0.1 g/ml), and clarified by centrifugation. The viral titers in the tissue samples were then determined by limiting dilution on chicken DF-1 cells. The remaining 8 chickens in each group were observed daily for 10 days for changes in body weight, signs of disease, and mortality.

**Statistical analysis.** The significance of the data was assessed using GraphPad Prism, version 5, software. Data are presented as the means  $\pm$  standard errors of the means (SEM) and analyzed by one-way analysis of variance (ANOVA) (Dunnett's multiple-comparison test) of at least three independent experiments.

## ACKNOWLEDGMENTS

This work was supported by the National Natural Science Foundation of China (grants 31602092 and 31672528), the National Key Research and Development Program of China (2017YFD0501000 and 2017YFD0500400), the Science and Technology Development Program of Jilin Province (20160519011JH, 20170204034NY, and 20180201040NY), and Special Funds for Industrial Innovation of Jilin Province (2016C063).

Roy Curtiss III is a founder of Curtiss Healthcare, Inc., in Gainesville, FL, which is a biotechnology company developing vaccines against bacterial diseases of farm animals.

## REFERENCES

1. Ganar K, Das M, Sinha S, Kumar S. 2014. Newcastle disease virus: current status and our understanding. *Virus Res* 184:71–81. <https://doi.org/10.1016/j.virusres.2014.02.016>.
2. Rui Z, Juan P, Jingliang S, Jixun Z, Xiaoting W, Shouping Z, Xiaojiao L, Guozhong Z. 2010. Phylogenetic characterization of Newcastle disease virus isolated in the mainland of China during 2001–2009. *Vet Microbiol* 141:246–257. <https://doi.org/10.1016/j.vetmic.2009.09.020>.
3. Ji Y, Liu T, Du Y, Cui X, Yu Q, Wang Z, Zhang J, Li Y, Zhu Q. 2018. A novel genotype VII Newcastle disease virus vaccine candidate generated by mutation in the L and F genes confers improved protection in chickens. *Vet Microbiol* 216:99–106. <https://doi.org/10.1016/j.vetmic.2018.01.021>.
4. Park JK, Lee DH, Yuk SS, Tseren-Ochir EO, Kwon JH, Noh JY, Kim BY, Choi SW, Kang SM, Lee JB, Park SY, Choi IS, Song CS. 2014. Virus-like particle vaccine confers protection against a lethal Newcastle disease virus challenge in chickens and allows a strategy of differentiating infected from vaccinated animals. *Clin Vaccine Immunol* 21:360–365. <https://doi.org/10.1128/CVI.00636-13>.
5. Yang ZQ, Liu QQ, Pan ZM, Yu HX, Jiao XA. 2007. Expression of the fusion glycoprotein of Newcastle disease virus in transgenic rice and its immunogenicity in mice. *Vaccine* 25:591–598. <https://doi.org/10.1016/j.vaccine.2006.08.016>.
6. Sawant PM, Verma PC, Subudhi PK, Chaturvedi U, Singh M, Kumar R, Tiwari AK. 2011. Immunomodulation of bivalent Newcastle disease DNA vaccine induced immune response by co-delivery of chicken IFN- $\gamma$  and IL-4 genes. *Vet Immunol Immunopathol* 144:36–44. <https://doi.org/10.1016/j.vetimm.2011.07.006>.
7. Kong W, Brovold M, Koenenman BA, Clark-Curtiss J, Curtiss R, III. 2012. Turning self-destructing Salmonella into a universal DNA vaccine delivery platform. *Proc Natl Acad Sci U S A* 109:19414–19419. <https://doi.org/10.1073/pnas.1217554109>.
8. Wang F, Chen Q, Li S, Zhang C, Li S, Liu M, Mei K, Li C, Ma L, Yu X. 2017. Linear DNA vaccine prepared by large-scale PCR provides protective immunity against H1N1 influenza virus infection in mice. *Vet Microbiol* 205:124–130. <https://doi.org/10.1016/j.vetmic.2017.05.015>.
9. Zhao K, Rong G, Hao Y, Yu L, Kang H, Wang X, Wang X, Jin Z, Ren Z, Li Z. 2016. IgA response and protection following nasal vaccination of chickens with Newcastle disease virus DNA vaccine nanoencapsulated with Ag@SiO<sub>2</sub> hollow nanoparticles. *Sci Rep* 6:25720. <https://doi.org/10.1038/srep25720>.
10. Dowd KA, Ko SY, Morabito KM, Yang ES, Pelc RS, DeMaso CR, Castilho LR, Abbink P, Boyd M, Nityanandam R, Gordon DN, Gallagher JR, Chen X, Todd JP, Tsybovsky Y, Harris A, Huang YS, Higgs S, Vanlandingham DL, Andersen H, Lewis MG, De La Barrera R, Eckels KH, Jarman RG, Nason MC, Barouch DH, Roederer M, Kong WP, Mascola JR, Pierson TC, Graham BS. 2016. Rapid development of a DNA vaccine for Zika virus. *Science* 354:237–240. <https://doi.org/10.1126/science.aai9137>.
11. Griffin BD, Muthumani K, Warner BM, Majer A, Hagan M, Audet J, Stein DR, Ranadheera C, Racine T, De La Vega MA, Piret J, Kucas S, Tran KN, Frost KL, De Graff C, Soule G, Scharikow L, Scott J, McTavish G, Smid V, Park YK, Maslow JN, Sardesai NY, Kim JJ, Yao XJ, Bello A, Lindsay R, Boivin G, Booth SA, Kobasa D, Embury-Hyatt C, Safronetz D, Weiner DB, Koberinger GP. 2017. DNA vaccination protects mice against Zika virus-induced damage to the testes. *Nat Commun* 8:15743. <https://doi.org/10.1038/ncomms15743>.
12. Galvez-Cancino F, Roco J, Rojas-Colonelli N, Flores C, Murgas P, Cruz-Gomez S, Oyarce C, Varas-Godoy M, Sauma D, Lladser A. 2017. A short hairpin RNA-based adjuvant targeting NF- $\kappa$ B repressor I $\kappa$ B $\alpha$  promotes migration of dermal dendritic cells to draining lymph nodes and antitumor CTL responses induced by DNA vaccination. *Vaccine* 35:4148–4154. <https://doi.org/10.1016/j.vaccine.2017.06.041>.
13. Stenler S, Lundin KE, Hansen L, Petkov S, Mozafari N, Isagulians M, Blomberg P, Smith CIE, Goldenberg DM, Chang CH, Ljungberg K, Hinkula J, Wahren B. 2017. Immunization with HIV-1 envelope T20-encoding DNA vaccines elicits cross-clade neutralizing antibody responses. *Hum Vaccin Immunother* <https://doi.org/10.1080/21645515.2017.1338546>.
14. Kong W, Wanda SY, Zhang X, Bollen W, Ting SA, Roland KL, Curtiss R, III. 2008. Regulated programmed lysis of recombinant Salmonella in host tissues to release protective antigens and confer biological containment. *Proc Natl Acad Sci U S A* 105:9361–9366. <https://doi.org/10.1073/pnas.0803801105>.
15. Darquet AM, Cameron B, Wils P, Scherman D, Crouzet J. 1997. A new DNA vehicle for nonviral gene delivery: supercoiled minicircle. *Gene Ther* 4:1341–1349. <https://doi.org/10.1038/sj.gt.3300540>.
16. Bigger BW, Tolmachev O, Collombet JM, Fragkos M, Palaszewski I,

- Coutelle C. 2001. An araC-controlled bacterial cre expression system to produce DNA minicircle vectors for nuclear and mitochondrial gene therapy. *J Biol Chem* 276:23018–23027. <https://doi.org/10.1074/jbc.M010873200>.
17. Jechlinger W, Azimpour Tabrizi C, Lubitz W, Mayrhofer P. 2004. Minicircle DNA immobilized in bacterial ghosts: in vivo production of safe non-viral DNA delivery vehicles. *J Mol Microbiol Biotechnol* 8:222–231. <https://doi.org/10.1159/000086703>.
  18. Kay MA, He CY, Chen ZY. 2010. A robust system for production of minicircle DNA vectors. *Nat Biotechnol* 28:1287–1289. <https://doi.org/10.1038/nbt.1708>.
  19. Van Duyn GD. 2015. Cre Recombinase. *Microbiol Spectr* 3:MDNA3-0014-2014. <https://doi.org/10.1128/microbiolspec.MDNA3-0014-2014>.
  20. Sgolastra F, Backlund CM, Ilker Ozay E, deRonde BM, Minter LM, Tew GN. 2017. Sequence segregation improves non-covalent protein delivery. *J Control Release* 254:131–136. <https://doi.org/10.1016/j.jconrel.2017.03.387>.
  21. Bi P, McAnally JR, Shelton JM, Sanchez-Ortiz E, Bassel-Duby R, Olson EN. 2018. Fusogenic micropeptide Myomixer is essential for satellite cell fusion and muscle regeneration. *Proc Natl Acad Sci U S A* 115:3864–3869. <https://doi.org/10.1073/pnas.1800052115>.
  22. Lambert JM, Bongers RS, Kleerebezem M. 2007. Cre-lox-based system for multiple gene deletions and selectable-marker removal in *Lactobacillus plantarum*. *Appl Environ Microbiol* 73:1126–1135. <https://doi.org/10.1128/AEM.01473-06>.
  23. Ghosh K, Guo F, Van Duyn GD. 2007. Synapsis of loxP sites by Cre recombinase. *J Biol Chem* 282:24004–24016. <https://doi.org/10.1074/jbc.M703283200>.
  24. Munye MM, Tagalakis AD, Barnes JL, Brown RE, McAnulty RJ, Howe SJ, Hart SL. 2016. Minicircle DNA provides enhanced and prolonged transgene expression following airway gene transfer. *Sci Rep* 6:23125. <https://doi.org/10.1038/srep23125>.
  25. Stenler S, Blomberg P, Smith CI. 2014. Safety and efficacy of DNA vaccines: plasmids vs. minicircles. *Hum Vaccin Immunother* 10:1306–1308. <https://doi.org/10.4161/hv.28077>.
  26. Stenler S, Wiklander OP, Badal-Tejedor M, Turunen J, Nordin JZ, Hallengard D, Wahren B, Andaloussi SE, Rutland MW, Smith CI, Lundin KE, Blomberg P. 2014. Micro-minicircle gene therapy: implications of size on fermentation, complexation, shearing resistance, and expression. *Mol Ther Nucleic Acids* 2:e140. <https://doi.org/10.1038/mtna.2013.67>.
  27. Dietz WM, Skinner NE, Hamilton SE, Jund MD, Heitfeld SM, Litterman AJ, Hwu P, Chen ZY, Salazar AM, Ohlfest JR, Blazar BR, Pennell CA, Osborn MJ. 2013. Minicircle DNA is superior to plasmid DNA in eliciting antigen-specific CD8<sup>+</sup> T-cell responses. *Mol Ther* 21:1526–1535. <https://doi.org/10.1038/mt.2013.85>.
  28. Schleef M, Schirmbeck R, Reiser M, Michel ML, Schmeer M. 2015. Minicircle: next generation DNA vectors for vaccination. *Methods Mol Biol* 1317:327–339. [https://doi.org/10.1007/978-1-4939-2727-2\\_18](https://doi.org/10.1007/978-1-4939-2727-2_18).
  29. Pang X, Ma F, Zhang P, Zhong Y, Zhang J, Wang T, Zheng G, Hou X, Zhao J, He C, Chen ZY. 2017. Treatment of human B-cell lymphomas using minicircle DNA vector expressing anti-CD3/CD20 in a mouse model. *Hum Gene Ther* 28:216–225. <https://doi.org/10.1089/hum.2016.122>.
  30. Gaspar VM, Baril P, Costa EC, de Melo-Diogo D, Foucher F, Queiroz JA, Sousa F, Pichon C, Correia IJ. 2015. Bioreducible poly(2-ethyl-2-oxazoline)-PLA-PEI-SS triblock copolymer micelles for co-delivery of DNA minicircles and doxorubicin. *J Control Release* 213:175–191. <https://doi.org/10.1016/j.jconrel.2015.07.011>.
  31. Gaspar VM, Goncalves C, de Melo-Diogo D, Costa EC, Queiroz JA, Pichon C, Sousa F, Correia IJ. 2014. Poly(2-ethyl-2-oxazoline)-PLA-g-PEI amphiphilic triblock micelles for co-delivery of minicircle DNA and chemotherapeutics. *J Control Release* 189:90–104. <https://doi.org/10.1016/j.jconrel.2014.06.040>.
  32. Li F, Cheng L, Murphy CM, Reszka-Blanco NJ, Wu Y, Chi L, Hu J, Su L. 2016. Minicircle HBV cccDNA with a *Gaussia luciferase* reporter for investigating HBV cccDNA biology and developing cccDNA-targeting drugs. *Sci Rep* 6:36483. <https://doi.org/10.1038/srep36483>.
  33. Wang Q, Jiang W, Chen Y, Liu P, Sheng C, Chen S, Zhang H, Pan C, Gao S, Huang W. 2014. In vivo electroporation of minicircle DNA as a novel method of vaccine delivery to enhance HIV-1-specific immune responses. *J Virol* 88:1924–1934. <https://doi.org/10.1128/JVI.02757-13>.
  34. Wang K, Jin Q, Ruan D, Yang Y, Liu Q, Wu H, Zhou Z, Ouyang Z, Liu Z, Zhao Y, Zhao B, Zhang Q, Peng J, Lai C, Fan N, Liang Y, Lan T, Li N, Wang X, Wang X, Fan Y, Doevendans PA, Sluijter JPG, Liu P, Li X, Lai L. 2017. Cre-dependent Cas9-expressing pigs enable efficient in vivo genome editing. *Genome Res* 27:2061–2071. <https://doi.org/10.1101/gr.222521.117>.
  35. Heger K, Kober M, RieB D, Drees C, de Vries I, Bertossi A, Roers A, Sixt M, Schmidt-Supprian M. 2015. A novel Cre recombinase reporter mouse strain facilitates selective and efficient infection of primary immune cells with adenoviral vectors. *Eur J Immunol* 45:1614–1620. <https://doi.org/10.1002/eji.201545457>.
  36. He L, Li Y, Li Y, Pu W, Huang X, Tian X, Wang Y, Zhang H, Liu Q, Zhang L, Zhao H, Tang J, Ji H, Cai D, Han Z, Han Z, Nie Y, Hu S, Wang QD, Sun R, Fei J, Wang F, Chen T, Yan Y, Huang H, Pu WT, Zhou B. 2017. Enhancing the precision of genetic lineage tracing using dual recombinases. *Nat Med* 23:1488–1498. <https://doi.org/10.1038/nm.4437>.
  37. Lallemand Y, Luria V, Haffner-Krausz R, Lonai P. 1998. Maternally expressed PGK-Cre transgene as a tool for early and uniform activation of the Cre site-specific recombinase. *Transgenic Res* 7:105–112. <https://doi.org/10.1023/A:1008868325009>.
  38. Li MZ, Elledge SJ. 2005. MAGIC, an in vivo genetic method for the rapid construction of recombinant DNA molecules. *Nat Genet* 37:311–319. <https://doi.org/10.1038/ng1505>.
  39. Ribeiro S, Mairhofer J, Madeira C, Diogo MM, Lobato da Silva C, Monteiro G, Grabherr R, Cabral JM. 2012. Plasmid DNA size does affect nonviral gene delivery efficiency in stem cells. *Cell Reprogram* 14:130–137. <https://doi.org/10.1089/cell.2011.0093>.
  40. Wang S, Li Y, Shi H, Sun W, Roland KL, Curtiss R, III. 2011. Comparison of a regulated delayed antigen synthesis system with in vivo-inducible promoters for antigen delivery by live attenuated *Salmonella* vaccines. *Infect Immun* 79:937–949. <https://doi.org/10.1128/IAI.00445-10>.
  41. Villaverde A, Benito A, Viaplana E, Cubarsi R. 1993. Fine regulation of cI857-controlled gene expression in continuous culture of recombinant *Escherichia coli* by temperature. *Appl Environ Microbiol* 59:3485–3487.
  42. Li L, Saade F, Petrovsky N. 2012. The future of human DNA vaccines. *J Biotechnol* 162:171–182. <https://doi.org/10.1016/j.jbiotec.2012.08.012>.
  43. van Diepen MT, Chapman R, Douglass N, Galant S, Moore PL, Margolin E, Ximba P, Morris L, Rybicki EP, Williamson AL. 2019. Prime-boost immunizations with DNA, modified vaccinia virus Ankara, and protein-based vaccines elicit robust HIV-1 tier 2 neutralizing antibodies against the CAP256 superinfecting virus. *J Virol* 93:e02155-18. <https://doi.org/10.1128/JVI.02155-18>.
  44. Asbach B, Kibler KV, Kostler J, Perdiguero B, Yates NL, Stanfield-Oakley S, Tomaras GD, Kao SF, Foulds KE, Roederer M, Seaman MS, Montefiori DC, Parks R, Ferrari G, Forthal DN, Phogat S, Tartaglia J, Barnett SW, Self SG, Gottardo R, Cristillo AD, Weiss DE, Galmin L, Ding S, Heeney JL, Esteban M, Jacobs BL, Pantaleo G, Wagner R. 2019. Priming with a potent HIV-1 DNA vaccine frames the quality of immune responses prior to a poxvirus and protein boost. *J Virol* 93:e01529-18. <https://doi.org/10.1128/JVI.01529-18>.
  45. Jiang Y, Kong Q, Roland KL, Curtiss R, III. 2014. Membrane vesicles of *Clostridium perfringens* type A strains induce innate and adaptive immunity. *Int J Med Microbiol* 304:431–443. <https://doi.org/10.1016/j.ijmm.2014.02.006>.
  46. Siebenkotten G, Leyendeckers H, Rainer C, Radbruch A. 1995. Isolation of plasmid DNA from mammalian cells with QIAPrep kit. *QIAGEN News* 2:11–12.
  47. James MB, Giorgio TD. 2000. Nuclear-associated plasmid, but not cell-associated plasmid, is correlated with transgene expression in cultured mammalian cells. *Mol Ther* 1:339–346. <https://doi.org/10.1006/mthe.2000.0054>.
  48. Cohen RN, van der Aa MA, Macaraeg N, Lee AP, Szoka FC, Jr. 2009. Quantification of plasmid DNA copies in the nucleus after lipoplex and polyplex transfection. *J Control Release* 135:166–174. <https://doi.org/10.1016/j.jconrel.2008.12.016>.
  49. Konjufca V, Wanda SY, Jenkins MC, Curtiss R, III. 2006. A recombinant attenuated *Salmonella enterica* serovar Typhimurium vaccine encoding *Eimeria acervulina* antigen offers protection against *E. acervulina* challenge. *Infect Immun* 74:6785–6796. <https://doi.org/10.1128/IAI.00851-06>.
  50. Miller PJ, Estevez C, Yu Q, Suarez DL, King DJ. 2009. Comparison of viral shedding following vaccination with inactivated and live Newcastle disease vaccines formulated with wild-type and recombinant viruses. *Avian Dis* 53:39–49. <https://doi.org/10.1637/8407-071208-Reg.1>.
  51. Kumar S, Nayak B, Collins PL, Samal SK. 2011. Evaluation of the Newcastle disease virus F and HN proteins in protective immunity by using a recombinant avian paramyxovirus type 3 vector in chickens. *J Virol* 85:6521–6534. <https://doi.org/10.1128/JVI.00367-11>.